Formation of intermediate-mass black holes as primordial black holes in the inflationary cosmology with running spectral index

Toshihiro Kawaguchi[1], Masahiro Kawasaki[2,3], Tsutomu Takayama[2,⋆], Masahide Yamaguchi[1] and Jun'ichi Yokoyama[4,3]

[1] *Department of Physics and Mathematics, Aoyama Gakuin University, Sagamihara 229-8558, Japan*
[2] *Institute for Cosmic Ray Research (ICRR), The University of Tokyo, Kashiwa 277-8582, Japan*
[3] *Institute for the Physics and Mathematics of the Universe, The University of Tokyo, Kashiwa 277-8582, JAPAN*
[4] *Research Center for the Early Universe (RESCEU), Graduate School of Science, The University of Tokyo, Tokyo 113-0033, Japan*

29 July 2014

ABSTRACT
Formation of primordial black holes (PBHs) on astrophysical mass scales is a natural consequence of inflationary cosmology if the primordial perturbation spectrum has a large and negative running of the spectral index as observationally suggested today, because double inflation is required to explain it and fluctuations on some astrophysical scales are enhanced in the field oscillation regime in between. It is argued that PBHs thus produced can serve as intermediate-mass black holes (IMBHs) which act as the observed ultraluminous X-ray sources (ULXs) by choosing appropriate values of the model parameters in their natural ranges. Our scenario can be observationally tested in near future because the mass of PBHs is uniquely determined once we specify the values of the amplitude of the curvature perturbation, spectral index and its running on large scales.

Key words: cosmology: theory – early universe – black hole physics.

1 INTRODUCTION

Ultraluminous X-ray sources (ULXs; Makishima et al. 2000) are characterized by their luminosity greater than $\sim 10^{39}$erg s^{-1} (well above the Eddington luminosity of a neutron star) and off-nuclear location in nearby galaxies (Fabbiano 1989; Colbert & Mushotzky 1999). In addition, X-ray variability on various timescales are found for some ULXs (Matsumoto & Tsuru 1999; Ptak & Griffiths 1999; Kaaret et al. 2001; Kubota et al. 2001). Luminosity, time variability and X-ray spectra of ULXs indicate that ULXs are accreting black holes, rather than young supernova remnants (Kaaret et al. 2001). Although association of ULXs with active star-forming regions are clearly shown (Matsushita et al. 2000; Zezas et al. 2002), the physical reason behind the association, and moreover the origin of ULXs, are still unclear.

The number density of ULXs can be roughly estimated as follows. Late-type/starburst galaxies hosting numerous compact X-ray sources (mostly high-mass X-ray binaries) within about 30Mpc from the Milky Way are listed in (Grimm, Gilfanov & Sunyaev, 2003). The number of these X-ray sources with each luminosity greater than

2×10^{38}erg s^{-1} is about 100. Grimm et al. also show that the luminosity function $N(L)$ of compact X-ray sources, which is defined as a number of X-ray sources with luminosity greater than L, is universal for galaxies if it is normalized proportionally to the star-forming rate (SFR). The normalized luminosity function tells that among $L > 10^{38.5}$erg s^{-1} sources about one-third have $L > 10^{39}$erg s^{-1}. Hence, the number of ULXs with $L > 10^{39}$erg s^{-1} will be $\sim$30 within 30 Mpc. Thus, the number density of ULXs is estimated to be $10^{-3.5}$Mpc^{-3}.

In spite of observational evidences, theoretical explanations of ULXs are still in dispute. The most challenging fact is the high luminosity greater than the Eddington luminosity of a stellar-mass black hole with mass $\sim 10 M_\odot$. For example, it is argued that sources of ULXs can be standard stellar-mass black holes with jets or relativistic beaming (Koerding, Falcke & Markoff 2002). Another possibility is stellar-mass black holes radiating at super-Eddington luminosities due to efficient photon leakage from accretion disks (e.g., Begelman 2002; Meyer 2004) and/or due to super-Eddington accretion rates ("slim accretion disks"; Abramowicz et al. 1988). Detailed computations of slim accretion disks (Kawaguchi 2003) indeed account for observed

X-ray spectra of ULXs (Okajima, Ebisawa & Kawaguchi 2006; Vierdayanti et al. 2006; Ebisawa & Kawaguchi 2006; Foschini et al. 2006).

ULXs can also be explained as sub-Eddington accretors by assuming black holes heavier than stellar-mass black holes (see Miller & Colbert 2004 and reference therein). Moreover, ULXs exhibit quasi-periodic oscillations (QPOs) at frequencies lower than the QPO frequencies of normal black hole binaries by a couple of orders (Strohmayer & Mushotzky 2003; Strohmayer et al. 2007). A straightforward interpretation of the longer timescales is a heavier black hole mass than $10 M_\odot$. Hence, intermediate-mass black holes (IMBHs) with mass $\sim 10^{2-4} M_\odot$ are considered to be one of the best candidates of ULXs.

The most challenging problem with such IMBHs is their formation mechanism. There are several possible mechanisms discussed so far. For instance, detailed evolution models of stellar binaries show that the generation rate of IMBHs is very small (Madhusudhan et al. 2006).

A promising possibility is that IMBHs could be remnants of Population III stars (e.g., Schneider et al. 2002). It is suggested that zero-metalicity stars form with masses $10^{2-3} M_\odot$ (e.g., Omukai et al. 2005). If the initial mass of a star is sufficiently large, it can collapse directly to an IMBH. These IMBHs can explain the observed number of ULXs if they are generated in galactic disks (Krolik 2004). It is also discussed that IMBHs produced in galactic halos can account for observed ULXs if Population III star formation is very efficient (Mii & Totani 2005). This possibility is suggested by the excess of the cosmic near-infrared background radiation (Wright & Reese 2000; Cambresy et al. 2001; Matsumoto et al. 2005). Note, however, that with the typical baryonic fraction of Pop-III stars, $f \sim 10^{-5}$ (Madau & Rees 2001), the abundance of remnants BHs, $\Omega_{\rm BH} = f \Omega_b \sim 4 \times 10^{-7}$, would be too small to account for IMBHs as we will see below (§4). On the other hand, if we assume a larger baryonic fraction, $f \gtrsim 10^{-3}$, then the Universe may have been reionised too early (Daigne et al. 2006).

Black holes can be produced via the collapse of overdense region of the early universe with large initial curvature fluctuation (Carr 1975). These black holes are called primordial black holes (PBHs). If the power spectrum of initial curvature perturbation has strong peak at a specific scale, collapse takes place at the epoch when this scale enters the horizon. Typical mass of resultant PBHs can be determined by the horizon mass in this epoch. Formation of PBHs in inflationary cosmology is discussed in (Ivanov 1997; Yokoyama 1997; Kawasaki et al. 1998; Yokoyama 1998a,b; Kawasaki & Yanagida 1999; Yamaguchi 2001).

One exotic possibility is the formation of IMBHs during Quantum Chromo Dynamics (QCD) phase transition (Jedamzik 1997, 1998; Jedamzik & Niemeyer 1999), if the transition is first order. Since the equation of state of the universe is relatively soft in this epoch, collapse of overdense region takes place easily. However, the horizon mass at this epoch is only $\mathcal{O}(1) M_\odot$ rather than $10^{2-4} M_\odot$.

In this paper, we present a model of inflation (Yamaguchi & Yokoyama 2004; Kawasaki et al. 2006) which can produce significant amount of PBHs in astrophysically interesting mass scales, to show that the origin of IMBHs could be such PBHs. In this scenario, the spectrum of initial curvature perturbation has strong peak due to the parametric resonance (Kofman et al. 1994, 1997; Shtanov et al. 1995). After inflation, the oscillation of the inflaton condensate can result in oscillating effective mass of another scalar field and/or the inflaton itself. This oscillating effective mass excites large fluctuations of that scalar field for specific modes. If this scalar field contributes to the energy density of the universe, excited fluctuation results in large curvature perturbation for this specific modes. If this curvature perturbation is sufficiently large, PBHs are produced via gravitational collapse (Green & Malik 2001; Bassett & Tsujikawa 2001). In general, characteristic scales of fluctuations excited by parametric resonance corresponds to very short wavelength compared to present observable scale. However, because another inflation is required after the parametric resonance in our model, these large fluctuations are naturally expanded to cosmologically and/or astronomically relevant scales.

Interestingly, this scenario is related to the running spectral index of the universe. Although it is not compelling, the result of the Wilkinson Microwave Anisotropy Probe (WMAP) observations (Komatsu et.al. 2008) indicates that the running of spectral index may be large and negative. These large running of the spectral index cannot be explained unless two or more successive inflations are assumed (Kawasaki et al. 2003; Easther & Peiris 2006). Therefore, if a large running spectral index is confirmed by forthcoming observations of cosmic microwave background (CMB), strongly peaked initial curvature perturbation from multiple inflation can be an interesting candidate of the formation mechanism of IMBH.

This paper is organized as follows. In Section 2, we explain the scenario of inflation and how the strongly peaked initial fluctuation is produced. The calculation of the mass distribution of PBHs is given in Section 3. In Section 4, we estimate the amount of IMBHs produced via the collapse of over dense region. In Section 5, we discuss the relation between the running spectral index and the typical mass of PBHs. The possibility of explaining other astronomically interesting PBHs is also discussed. Finally, we summarise the results.

2 GENERATION OF PEAKED POWER SPECTRUM OF INITIAL CURVATURE PERTURBATION VIA A DOUBLE INFLATION MODEL

2.1 Smooth hybrid new inflation model

The power spectrum of initial curvature perturbation is needed to be strongly peaked in order to result in the formation of relevant amount of PBHs via collapse of overdense region. Initial curvature perturbation is determined by the detail of inflation. Here we consider the smooth hybrid new inflation model in supergravity proposed by Yamaguchi & Yokoyama (2004). It was first considered to account for the running spectral index suggested by WMAP. The spectral index n of the initial curvature perturbation $\mathcal{P}_\mathcal{R}$ is suggested to be dependent on the comoving wavenumber k, according to the result of WMAP observation. The best-fit values of the amplitude $\mathcal{P}_\mathcal{R}$, spectral index n and its

running $\alpha \equiv dn/d\ln k$ at the pivot scale $k_0 = 0.002 \mathrm{Mpc}^{-1}$ are

$$\begin{aligned} \mathcal{P_R} &= (2.40 \pm 0.11) \times 10^{-9}, \quad n = 1.031^{+0.054}_{-0.055}, \\ \alpha &= -0.037 \pm 0.028 \end{aligned} \tag{1}$$

by the WMAP 5 year result only (Komatsu et.al. 2008). This suggests the existence of large running from $n > 1$ at long wavelength scale to $n < 1$ at short wavelength scale within the range WMAP observation can probe, namely, $1 \mathrm{Mpc} \lesssim k^{-1} \lesssim 10^4 \mathrm{Mpc}$.

In our model, two inflatons are introduced and two stages of inflation takes place in succession. (See Kawasaki et al. (2006) for the more detailed discussions based on supergravity.) At first, the smooth hybrid inflation occurs. This inflation is characterized by the following effective potential of an inflaton real scalar field σ,

$$V(\sigma) = \begin{cases} \mu^4 \left[1 - \dfrac{2}{27} \dfrac{(\mu M)^2}{\sigma^4} + \dfrac{\sigma^4}{8 M_G^4} \right] & \text{for } \sigma \gg (\mu M)^{\frac{1}{2}} \\[4mm] \dfrac{8\mu^3}{M} \sigma^2 & \text{for } \sigma \ll (\mu M)^{\frac{1}{2}} \end{cases} \tag{2}$$

Here parameters with dimension of mass μ and M indicate the energy scale of smooth hybrid inflation and the cut-off scale of the underlying theory, respectively. Here M_G is the reduced Planck mass, $M_G = 2.4 \times 10^{18} \mathrm{GeV}$. Typically, parameters μ and M satisfy $\mu \ll M \lesssim M_G$. The inflaton σ slowly rolls from $\sigma \gg (\mu M)^{1/2}$ to $\sigma = 0$. Here you should notice that the observational quantities $\mathcal{P_R}$, n, and α at the pivot scale k_0 of primordial fluctuations are completely determined by the model parameters μ, M, and $\sigma = \sigma_0$ at the moment the scale k_0 exits the horizon. The duration of the smooth hybrid inflation after the scale k_0 exits the horizon is also determined once σ_ini, μ, and M are specified.

Smooth hybrid inflation model is a variant of hybrid inflation model. In both models inflation is driven by a false vacuum energy of some symmetry-breaking field. In hybrid inflation, the restored symmetry is broken only at the end of inflation resulting in formation of topological defects which could be cosmologically harmful. On the other hand, during smooth hybrid inflation, by virtue of non-renormalizable terms, symmetry remains broken and there is no defects formation at the end of inflation. These non-renormalizable terms can also serve to produce appreciable negative running spectral index. Furthermore, while it has been shown that hybrid inflation requires severe fine-tuning of initial condition, (Tetradis N. 1998; Mendes L. E. 2000) smooth hybrid inflation is free from such a fine tuning and can be realized naturally.

The most important feature of this inflation model is that the largely running spectral index can be realized. This potential has positive curvature for larger σ and negative curvature for smaller σ. Since the spectral index of the initial curvature perturbation depends on the gradient of the potential, this inflation results in scale-dependent spectral index. Large wavelength modes of the initial curvature perturbation are produced while the inflaton takes a large value. Therefore, the spectral index for these modes is larger than unity. On the other hand, short wavelength modes are produced while the inflaton takes a smaller value. Thus, the spectral index for these modes is smaller than unity. Consequently, negative running of the spectral index suggested

by the WMAP 5 year result can be realized. For example, a parameter choice (equations are corrected)

$$\mu = 2.1 \times 10^{-3} M_G, \ M = 1.3 M_G, \ \sigma_0 = 0.227 M_G \tag{3}$$

gives

$$\begin{aligned} \mathcal{P_R} &= 2.40 \times 10^{-9}, \quad n = 1.040, \\ \alpha &= -0.033, \end{aligned} \tag{4}$$

which is in the range (1). However, since large running needs large variation of the gradient of the potential, the evolution of inflaton must be very fast in order to account for the large running of the spectral index, which implies that smooth hybrid inflation does not last so long. Thus, another inflation is necessary to push the relevant scales to cosmologically observable scale.

In this model, new inflation is considered as another inflation to compensate for the duration of the inflationary epoch. Moreover, it naturally leads to low reheating temperature to avoid the overproduction of the gravitinos. The effective potential of the second inflaton field ϕ during this new inflation is given by

$$V(\phi) = v^4 - \frac{c}{2} \frac{v^4 \phi^2}{M_G^2} - \frac{g}{2} \frac{v^2 \phi^4}{M_G^2} + \frac{g^2}{16} \frac{\phi^8}{M_G^4}, \tag{5}$$

where v determines the scale of new inflation, which is assumed to be $v \ll \mu$. Parameters $c \lesssim 1$ and $g < 1$ determine the shape of the potential $V(\phi)$. In addition, the second inflaton field ϕ is coupled to σ through gravitationally suppressed interactions in supergravity even if no direct coupling is introduced. Since the contribution from this coupling dominates the potential of ϕ, ϕ is trapped to a value close to, but different from $\phi = 0$, while σ has a non-vanishing value. After the smooth hybrid inflation, σ oscillates around $\sigma = 0$ with its amplitude decreasing. Eventually, the contribution from $V(\phi)$ becomes dominant, and then ϕ begins to roll slowly from the vicinity of $\phi = 0$ to the minimum $\phi \simeq (4v^2 M_G^2/g)^{1/4}$. The duration of new inflation is determined by parameters v, g, and c. Note that fluctuation generated during the new inflation is not constrained by observations unless it is extremely large, because length scale of such fluctuation is too small to be cosmologically observable. The exception is the strong fluctuation generated via the parametric resonance (Kawasaki et al. 2006), which may serve as a seed of PBHs, as discussed below.

2.2 Generation of strong fluctuation via the parametric resonance

Because of the self-coupling of σ, oscillating condensate of σ gives oscillating contribution to its own effective mass. Since this self-coupling is large, the amplitude of this oscillating contribution is larger than its mass at the origin $m_\sigma \simeq (8\mu^3/M)^{1/2}$. Hence some specific modes of fluctuation of σ are strongly amplified via the parametric resonance. In our case, it is determined by the evolution equation of Fourier modes of fluctuation σ_k, which can be approximated as

$$\sigma_k'' + [A - 2q\cos(2z)]\,\sigma_k = 0. \tag{6}$$

Here A is a function of $k/(am_\sigma)$, where a is the scale factor. q is a time-dependent parameter proportional to the

self-coupling and the amplitude of the oscillation of the zero-mode of σ. The prime represents derivative with respect to the time variable z defined by the proper time as $2z = m_\sigma t - \pi/2$. Equation (6) has the shape of Mathieu equation. The solution of this equation have infinite sequence of instability bands determined by the value of A. In these instability bands, the solution grows exponentially for $q \gtrsim 1$. Hence, the modes k satisfying the condition $k/a = m_\sigma \times (const.)$ grows exponentially. According to numerical calculation, the strongest instability appears at around $k/a = m_\sigma \times \mathcal{O}(10^{-1})$. Note that the comoving scale k in this instability band is inside the horizon at the beginning of the new inflation. Eventually q decreases to $q \ll 1$ and the parametric resonance ceases. Later, fluctuations ϕ_k with the same range of k get large amplitudes via linear coupling with the amplified fluctuation σ_k. These fluctuations ϕ_k determine the curvature perturbation during the new inflation. Thus, the curvature perturbation has a large amplitude at a specific range of k.

We can see that the position of the strong peak k_p is approximately determined by the factor (μM) and the duration of the smooth hybrid inflation. The peak position k_p satisfies

$$\frac{k_p}{a_e} \simeq C m_\sigma, \tag{7}$$

where $C \simeq \mathcal{O}(10^{-1})$ is determined by the detail of the parametric resonance and a_e is the scale factor at the end of the smooth hybrid inflation. On the other hand, the scale factor a_0 at the moment the pivot scale exits the horizon and the Hubble parameter during the smooth hybrid inflation, $H_s \sim \mu^2/(\sqrt{3}M_G)$, satisfies

$$\frac{k_0}{a_0 H_s} = 1. \tag{8}$$

Therefore, we get

$$\ln \frac{k_p}{k_0} = \ln \frac{a_e}{a_0} + \ln \frac{M_G}{\sqrt{\mu M}} + \ln C + 1.6. \tag{9}$$

The shorter smooth hybrid inflation we assume, the larger-mass PBHs are produced.

Note that the typical mass of PBHs is determined once we specified $\mathcal{P}_\mathcal{R}$, n and α. In our model, only the smooth-hybrid inflation is responsible to the curvature perturbation of cosmologically interesting scales. Since free parameters of our smooth-hybrid inflation model are μ, M and the value of inflaton σ_0 at the moment the pivot scale k_0 crosses outside the horizon, cosmological parameters $\mathcal{P}_\mathcal{R}$, n and α depend only on parameters μ, M and σ_0. Therefore, in order to reproduce specific values of $\mathcal{P}_\mathcal{R}$, n and α, we look for appropriate values of μ, M and σ_0. Once we find them, a_e/a_0 is determined by the dynamics of the inflaton, and then k_p/k_e is specified by the Eq.(9).

The amount of PBHs depends on the height of the peak, which is determined by the balance of the efficiencies of the parametric resonance and the subsequent decay of σ into lighter particles. If this decay rate is sufficiently large, it makes the parametric resonance weaker. It is extremely difficult to estimate the magnitude of this strong peak analytically because of the non-perturbative nature of the parametric resonance.
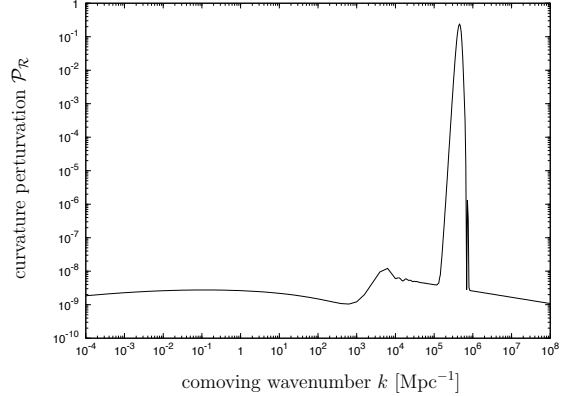
Figure 1. The spectrum leading to the formation of IMBHs from the smooth hybrid new inflation model.

2.3 Spectrum of the curvature perturbation for the formation of IMBHs

In Fig.1, we show an example of the spectrum of the initial curvature perturbation which results in the formation of significant amount of IMBHs. In order to give a example of generation of $10^2 M_\odot$ PBHs, we choose $\mu = 1.6 \times 10^{-3} M_G$, $M = 0.81 M_G$, $v = \mu/4$, $c = 0.1$, and $g = 10^{-6}$ for parameters of the smooth hybrid new inflation as an example. The position of the peak is at $k_p = 4.4 \times 10^5 \text{Mpc}^{-1}$, thus the typical mass of resultant black holes is estimated as $M_{\text{PBH}} = 108 M_\odot$ by the horizon mass at the moment the scale k_p enters the horizon. Unfortunately, it is difficult to estimate the range of these parameters which results $M_{\text{PBH}} \sim 100 M_\odot$. As a hint for this estimation, we tried various parameters for μ and M. For example, $\mu = 1.7 \times 10^{-3} M_G$ and $M = 0.86 M_G$ gives $M_{\text{PBH}} \simeq 1000 M_\odot$, while $\mu = 1.5 \times 10^{-3} M_G$ and $M = 0.72 M_G$ gives $M_{\text{PBH}} \simeq 10 M_\odot$, both reproducing the cosmological parameters consistent with (1). We also assumed the decay rate of σ as $\Gamma = 7.65 \times 10^{-8} M_G$. Modes of curvature perturbation with $k < 10^3 \text{Mpc}^{-1}$ are generated during the smooth hybrid inflation. This spectrum gives $\mathcal{P}_\mathcal{R} = 2.4 \times 10^{-9}$, $n = 1.067$, and $\alpha = -0.014$ at $k_0 = 0.002 \text{Mpc}^{-1}$. A large and negative running spectral index is a characteristic feature of formation of IMBHs via this scenario, which can be tested by forthcoming observations of CMB.

3 FORMATION OF PRIMORDIAL BLACK HOLES VIA COLLAPSE OF OVERDENSE REGION

PBHs were considered to be produced via gravitational collapse if the density perturbation $\delta \equiv \delta\rho/\rho$ within a patch of the universe is larger than some critical value δ_c at the moment the Hubble radius becomes smaller than the size of the patch (Carr 1975). Later, a critical phenomenon was observed (Niemeyer & Jedamzik 1998) in the formation of PBHs via gravitational collapse of radiation fluid in the Friedmann-Robertson-Walker background (Evans & Coleman 1994). According to (Niemeyer & Jedamzik 1998), the mass of PBH M_{PBH} produced via collapse of a overdense region with the density

perturbation δ has a scaling relation

$$M_{\rm PBH} = \kappa M_H (\delta - \delta_c)^{\gamma}, \qquad (10)$$

where M_H is the horizon mass at the moment this region enters the horizon. The index γ and the critical value δ_c are universal constants, which are estimated by numerical simulations as $\gamma \simeq 0.35$ and $\delta_c \simeq 0.67$, where the latter is quoted from results of numerical simulation of critical collapse(Niemeyer & Jedamzik 1999).

Given strongly peaked spectrum of curvature perturbation, the mass spectrum of PBHs is estimated as follows (Yokoyama 1998c; Barrau et al. 2003). Assuming that the initial curvature perturbation has a Gaussian probability distribution and that the curvature perturbation is strongly peaked, the differential mass spectrum of the PBHs at the time of formation can be given by.

$$\frac{d\Omega_{\rm PBH}(t_c)}{d\ln M_{\rm PBH}} = \epsilon^{-\frac{1}{\gamma}} \beta(M_H) \left(1 + \frac{1}{\gamma}\right) \left(\frac{M_{\rm PBH}}{M_H}\right)^{1+\frac{1}{\gamma}}$$
$$\times \exp\left[-\epsilon^{-\frac{1}{\gamma}}(1+\gamma)\left(\frac{M_{\rm PBH}}{M_H}\right)^{\frac{1}{\gamma}}\right]. \quad (11)$$

The parameter ϵ is defined as the ratio of the peak of differential mass spectrum $M_{\rm max}$ to the horizon mass M_H. The function $\beta(M_H)$ is the probability that the relevant mass scale has an above-threshold amplitude of fluctuations to collapse as it enters the Hubble radius, namely,

$$\beta(M_H) = \int_{\delta_c} p(\delta, t_c)d\delta \simeq \frac{\sigma_H(t_c)}{\sqrt{2\pi}\delta_c} \exp\left(-\frac{\delta_c^2}{2\sigma_H^2(t_c)}\right) \qquad (12)$$

where $p(\delta, t_c)$ is the probability distribution function of the density perturbation at the moment the scale k_p enters the particle horizon, which is assumed to be Gaussian. The variance of the density perturbation $\sigma_H(t_c)$ smoothed over the comoving length scale k_p^{-1} can be estimated by

$$\sigma_H^2(t_c) = \frac{16}{81} \int_p \left(\frac{k}{k_p}\right)^3 \mathcal{P}_{\mathcal{R}}(k) T^2\left(\frac{k}{k_p}, t_c\right) W_{\rm TH}^2\left(\frac{k}{k_p}\right) \frac{dk}{k_p}. \quad (13)$$

Here we employed the top-hat window function

$$W_{\rm TH}(x) = \frac{3}{x^2}\left(\frac{\sin x}{x} - \cos x\right). \qquad (14)$$

Note that the power spectrum of the density perturbation $\mathcal{P}_{\delta}$ is given by

$$\mathcal{P}_{\delta} = \frac{16}{81}\left(\frac{k}{k_p}\right)^4 T^2\left(\frac{k}{k_p}, t_c\right) \mathcal{P}_{\mathcal{R}}, \qquad (15)$$

where $T(k/k_p, t_c)$ is the transfer function which is given by

$$T\left(\frac{k}{k_p}, t_c\right) = \frac{k_p^2}{k^2}\left\{\frac{\sqrt{3}k_p}{k}\sin\left(\frac{k}{\sqrt{3}k_p}\right) - \cos\left(\frac{k}{\sqrt{3}k_p}\right)\right\}. \quad (16)$$

Finally, the differential mass spectrum of PBHs at present can be given by

$$\frac{d\Omega_{\rm PBH,0}}{d\ln M_{\rm PBH}} = \frac{d\Omega_{\rm PBH}(t_c)}{d\ln M_{\rm PBH}} \exp\left(\int_{t_c}^{t_0} 3wHdt\right) \qquad (17)$$

unless PBHs are dominant constituent of dark matter, where w is the effective equation-of-state parameter of the total cosmic energy density including contribution from dark energy. In Fig.2, we show the differential mass spectrum (17) calculated for the spectrum shown in Fig.1 with $\epsilon = 1$.
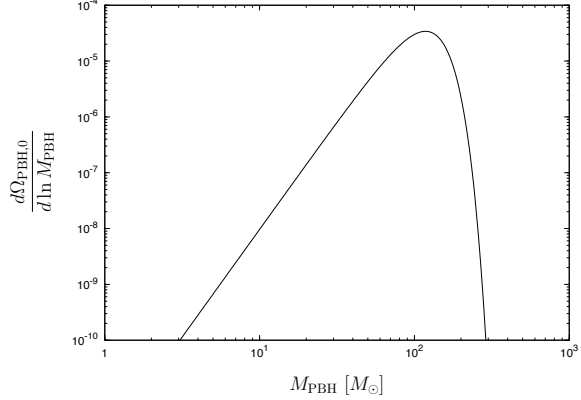
Figure 2. The differential mass spectrum (17) calculated for the spectrum shown in Fig.1.

We took contribution from dark energy into account. We can see that the mass distribution of PBHs is well peaked around $M_{\rm PBH} = 108 M_{\odot}$. Therefore, we can conclude that only IMBHs are produced from this spectrum.

4 AMOUNT OF IMBHS

The observational constraint on the total amount of IMBHs can be estimated from the observed number density of ULXs $10^{-3.5}{\rm Mpc}^{-3}$, as follows. Assuming that ULXs are IMBHs with typical mass $10^2 M_{\odot}$, this number density means that the contribution of IMBHs observed as ULXs to the density parameter of the universe $\Omega_{\rm ULXBH}$ is $\sim 10^{-12.5}$. Agol and Kamionkowski (2001) estimate the probability for floating black holes to acquire high enough accretion rates from interstellar medium as $\sim 10^{-5}$. Furthermore, if we consider the enhancement of dark matter (and IMBHs) in the galactic disk region properly, the typical mass fraction of dark matter (over the entire dark matter halo) within the galactic disk region would be $\sim 10^{-3}$ (see Mii & Totani 2005). By combining the above three points, we can then estimate the total abundance of the IMBHs in the universe as

$$\Omega_{\rm IMBH} \sim \Omega_{\rm ULXBH} \times (10^{-5} \times 10^{-3})^{-1} = 10^{-4.5}. \qquad (18)$$

We note that estimations adopted above would be valid only up to the order of magnitude.

We here point out that $\Omega_{\rm IMBH}$ quoted satisfies the constraints from CMB observations (see Ricotti, Ostriker & Mack 2007). Namely, if there are too many PBHs, a fraction of these black holes shining by gas accretion in the early universe at $z \approx 100 - 1000$ (where gas density is quite high) must have distorted the CMB spectrum. Then, the CMB spectral distortions (based on Far-Infrared Absolute Spectrophotometer (FIRAS) data) provide an upper limit for allowed $\Omega_{\rm IMBH}$ to be $10^{-4.5}$ for the case of the PBH mass $M_{\rm PBH} = 10^2 M_{\odot}$ (Ricotti et al. 2007).

We calculated the abundance of the IMBHs from the differential mass spectrum Eq.(17) for the same parameter set as we chose for Fig.1 and various decay rates Γ. The result is summarised in Fig.3, which shows that the abundance of IMBHs is sensitively dependent on the decay rate Γ. Accordingly, the range $7.65 \times 10^{-8} M_G < \Gamma < 7.74 \times 10^{-8} M_G$
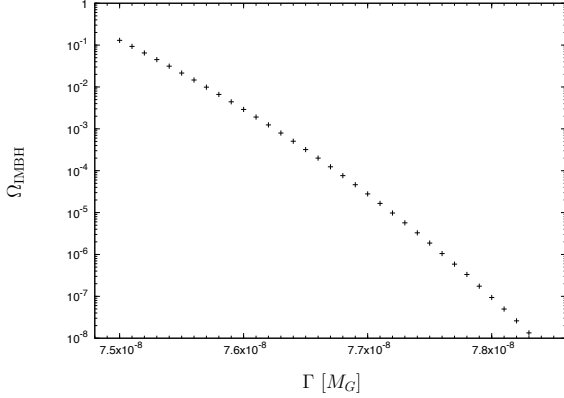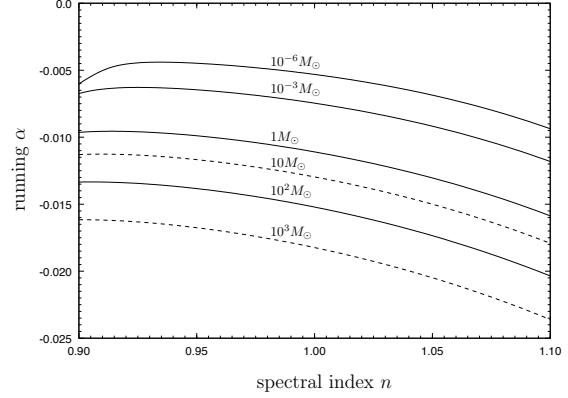
Figure 3. The relation between the abundance of IMBHs Ω_{IMBH} and the decay rate Γ.

Figure 4. Contour-lines of the typical mass of PBHs on the n-α plane.

results in the abundance $10^{-5.5} < \Omega_{\mathrm{IMBH}} < 10^{-3.5}$. Thus, this scenario needs tuning of the decay rate in order to account for the abundance of ULXs. This is simply due to the fact that the abundance of PBHs is exponentially sensitive to the peak amplitude of fluctuation, and all the other models of PBH formation requires the same level of fine tuning. Note that the decay rate of σ is expected to be given by $\Gamma \simeq N g_\sigma^2 m_\sigma / (8\pi)$ where g_σ is some gauge coupling constant included in near-Planck scale physics and N is the number of decay channels. Under the parameter set we have chosen, the above constraint on Γ is rewritten by $N g_\sigma^2 \sim 10^{-2}$, which can be satisfied by natural values of N and g_σ. Here one should notice that Γ has nothing to do with the reheating temperature after the final inflation, which is determined by the decay rate of ϕ.

5   SPECTRAL INDEX AND TYPICAL MASS OF PBHS

Here let us consider the relation between the typical mass of PBHs and cosmological parameters, spectral index and its running. As we discussed in the Section 2, $\mathcal{P}_\mathcal{R}$, n and α at the pivot scale $k_0 = 0.002\mathrm{Mpc}^{-1}$ are determined once we choose parameters μ, M and the value of σ at the moment the scale k_0 exits the horizon. This choice simultaneously determines the duration of the smooth hybrid inflation $\ln(a_e/a_0)$. Thus, if we fix the amplitude $\mathcal{P}_\mathcal{R}$ to be the best-fit value of the result of WMAP3, we can compute the mass of PBH for each combination of (n, α), up to an uncertainty in the detail of parametric resonance. A brief explanation of the method we used is given in Appendix.

In Fig.4, we show the relation[1] between typical mass of PBHs and the cosmological parameters n and α. We can see that larger mass PBHs requires larger running of the spectral index, while lower mass PBHs can be produced with negligible running. This can be understood by the fact that the

---

[1] Cosmological parameters n and α of the spectrum shown in Fig.1 and the typical mass of PBHs $108 M_\odot$ is deviated from this result. The main reason is that v is not negligibly small compared with μ. Since long oscillatory phase requires extremely long numerical calculation, we chose large v for our calculation.

short smooth hybrid inflation is realized for steep potential, which means large running. If we choose some other appropriate values of model parameters, this scenario can alternatively explain one of other astronomically interesting PBHs, such as $0.1 - 1 M_\odot$ BHs considered to be a candidate of massive compact halo objects (MACHOs) (Alcock et al. 2000) or 10^{15}g BHs which are possible sources of ultra high energy cosmic rays (UHECRs) (Takeda et al. 2003), although the latter possibility is probably no longer interesting given the recent Auger data (Abraham et al. 2007). The former requires $\alpha \sim -0.01$, while the latter requires negligibly small α. For the latter case, best-fit values of $\mathcal{P}_\mathcal{R}$ and n is given by

$$\mathcal{P}_\mathcal{R} = (2.41 \pm 0.11) \times 10^{-9}, \quad n = 0.963^{+0.014}_{-0.015} \qquad (19)$$

from the result of WMAP 5 year only, assuming $\alpha = 0$, which can also be realised in the present scenario.

6   SUMMARY AND DISCUSSION

We considered the formation of IMBHs as a candidate of ULXs via gravitational collapse of overdense region of the curvature perturbation whose spectrum is strongly peaked. This initial fluctuation is produced by a double inflation model, the smooth hybrid new inflation. The peak is originated from the amplification of specific modes of fluctuation via the parametric resonance. This inflation model can also explain the observed running spectral index. We found the relation between typical mass of PBHs and the cosmological parameters n and α. This result shows that the formation of IMBHs in this scenario requires significant running of the spectral index. The amount of IMBHs depends on the height of the peak, which is determined by the detail of parametric resonance and the decay rate of the inflaton. The decay rate must be some specific and fine-tuned value for required abundance of IMBHs. The level of required fine-tuning is no different from other models of PBH formation. What is important here is that the requirement can be satisfied with natural values of the parameters. This scenario can alternatively explain one of other PBHs, such as $0.1 - 1 M_\odot$ BHs considered to be candidates of MACHOs or 10^{15}g BHs which

are possible sources of UHECRs with some other appropriate choices of model parameters.

The production of strongly peaked initial curvature perturbation via the parametric resonance can take place in other double inflation models with intermediate oscillatory phases (Kawasaki et al. 2003; Yamaguchi & Yokoyama 2003). Since these double inflation models are required to explain the possible large running of the spectral index, observational confirmation of large and negative running spectral index may be regarded as a hint of IMBHs.

APPENDIX

Here we will explain how Fig.4 was determined. We used analytic estimations given in (Yamaguchi & Yokoyama 2004), because it is sufficient to see approximate dependence of $M_{\rm PBH}$ on (n, α).

According to (Yamaguchi & Yokoyama 2004), the dynamics of inflaton σ has characteristic values of σ. Namely, σ_d, where the dominant contribution to the dynamics changes from the second term in Eq.(2) to the third term, and σ_c, where the slow-roll condition is violated and the smooth hybrid inflation ends. These values are estimated by following equations. Note that we consider only the case $m = 2$ in (Yamaguchi & Yokoyama 2004).

$$\sigma_d = \left(\frac{16}{27}\right)^{\frac{1}{8}} \times \left(\frac{\mu M}{M_G^2}\right)^{\frac{1}{4}}, \tag{20}$$

$$\sigma_c = \left(\frac{40}{27}\right)^{\frac{1}{6}} \times \left(\frac{\mu M}{M_G^2}\right)^{\frac{1}{3}}. \tag{21}$$

The number of e-foldings N_d from $\sigma = \sigma_d$ to $\sigma = \sigma_c$ is

$$N_d = -\frac{5}{6} + \left(\frac{1}{48}\right)^{\frac{1}{4}} \times \left(\frac{\mu M}{M_G^2}\right)^{\frac{1}{2}}. \tag{22}$$

Now, if we choose the value of μM and require the typical mass of resultant PBHs $M_{\rm PBH}$, $N_e \equiv \ln(a_e/a_0)$ is determined by Eq.(9). Then, the value of σ_0, which is the value of σ at the moment the pivot scale k_0 crosses outside the horizon, is determined by tracing back the dynamics of σ from the end of smooth hybrid inflation $\sigma = \sigma_c$. If $N_e > N_f$, it means that $\sigma_0 > \sigma_d$. Therefore,

$$\sigma_0 = \left[\left\{\left(\frac{1}{48}\right)^{\frac{1}{4}} + \left(\frac{27}{16}\right)^{\frac{1}{4}}\right\}\left(\frac{\mu M}{M_G^2}\right)^{-\frac{1}{2}} - \frac{5}{6} - N_e\right]^{-\frac{1}{2}}. \tag{23}$$

On the other hand, if $N_e < N_f$, then $\sigma_0 < \sigma_d$ and

$$\sigma_0 = \left(\frac{5}{6} + N_e\right)^{\frac{1}{6}} \left(\frac{4}{3}\right)^{\frac{1}{3}} \left(\frac{\mu M}{M_G^2}\right)^{\frac{1}{3}}. \tag{24}$$

Thus, we can determine σ_0 if we specify (μM) and $M_{\rm PBH}$.

Because $\mathcal{P}_{\mathcal{R}}$ is given by

$$\mathcal{P}_{\mathcal{R}} = \frac{\mu^2 M_G}{\sqrt{3}\pi} \left\{\sigma_d^3 \left(\frac{\sigma_d}{\sigma_0}\right)^5 + \sigma_0^3\right\}^{-1}, \tag{25}$$

parameters μ, and then M, can be calculated once we determined σ_0. Cosmological parameters n and α are calculated via slow-roll parameters.

Consequently, if we choose $M_{\rm PBH}$, we can draw a curve on (μ, M) plane which results the typical mass of PBHs $M_{\rm PBH}$. Deriving the corresponding values of $(n, \alpha)|_{\sigma=\sigma_0}$, we can draw Fig.4.

REFERENCES

Abraham J. *et al.* [Pierre Auger Collaboration], 2007, arXiv:0712.1147 [astro-ph].

Abramowicz M. A., Czerny B., Lasota J. P., Szuszkiewicz E., 1988, ApJ, 332, 646

Agol E., Kamionkowski M., 2002, MNRAS, 334, 553

Alcock C. *et al.* [MACHO Collaboration], 2000, ApJ, 542, 281

Barrau A., Blais D., Boudoul G., Polarski D., 2003, Phys. Lett. B, 551, 218

Bassett B. A., Tsujikawa S., 2001, Phys. Rev. D, 63, 123503

Begelman M. C., 2002, ApJ, 568, L97

Cambresy L., Reach W. T., Beichman C. A., Jarrett T. H., 2001, ApJ, 555, 563

Carr B. J., 1975, ApJ, 201, 1

Colbert E. J. M., Mushotzky R. F., 1999, ApJ, 519, 89

Daigne, F., Olive, K. A., Silk, J., Stoehr, F., Vangioni, E., 2006 ApJ, 647, 773

Easther R., Peiris H., 2006, J. Cosmol. Astropart. Phys., 0609, 010

Ebisawa K., Kawaguchi T., 2006, Advances in Space Res., 38, 2862

Evans C. R., Coleman J. S., 1994, Phys. Rev. Lett., 72, 1782

Fabbiano G., 1989, ARA&A, 27, 87

Foschini L., et al., 2006, AdSpR, 38, 1378

Green A. M., Malik K. A., 2001, Phys. Rev. D, 64, 021301

Grimm H. J., Gilfanov M., Sunyaev R., 2003, MNRAS, 339, 793

Ivanov P., 1997 Phys. Rev. D, 57, 7145

Jedamzik K., 1997, Phys. Rev. D, 55, 5871

Jedamzik K., 1998, Phys. Rep., 307, 155

Jedamzik K., Niemeyer J. C., 1999, Phys. Rev. D, 59, 124014

Kaaret P., Prestwich A.H., Zezas A., Murray S. S., Kim D.-W., Kilgard R. E., Schlegel E. M., Ward M. J., 2001, Mon. Not. Roy. Astron. Soc. Lett., 321, L29

Kawaguchi T., 2003, ApJ, 593, 69

Kawasaki M., Sugiyama N., Yanagida T., 1998, Phys. Rev. D, 57, 6050

Kawasaki M., Yanagida T., 1999, Phys. Rev. D, 59, 043512

Kawasaki M., Yamaguchi M., Yokoyama J., 2003, Phys. Rev. D, 68, 023508

Kawasaki M., Takayama T., Yamaguchi M., Yokoyama J., 2006, Phys. Rev. D, 74, 043525

Koerding E., Falcke H., Markoff S., 2002, A&A, 382, L13

Kofman L., Linde A. D., Starobinsky A. A., 1994, Phys. Rev. Lett., 73, 3195

Kofman L., Linde A. D., Starobinsky A. A., 1997, Phys. Rev. D, 56, 3258

Komatsu E., et al. [WMAP Collaboration], 2008, arXiv:0803.0547 [astro-ph]

Krolik L. H., 2004, ApJ, 615, 383

Kubota A., Mizuno T., Makishima K., Fukazawa Y., Kotoku J., Ohnishi T., Tashiro M., 2001, ApJ, 547, L119

Madau P., Rees M. J., 2001, ApJ, 551, L27

Madhusudhan N., Justham S., Nelson L., Paxton B., Pfahl E., Podsiadlowski P., Rappaport S., 2006, ApJ, 640, 918

Makishima K. et al., 2000, ApJ, 535, 632

Matsumoto T. et al., 2005, ApJ, 626, 31

Matsumoto H., Tsuru T. G., 1999, PASJ, 51, 321

Matsushita S., Kawabe R., Matsumoto H., Tsuru T. G., Kohno K., Morita K. I., Okumura S. K., Vila-Vilaro B., 2000, ApJ, 545, L107

Mendes L. E., Liddle A. R., 2000, Phys. Rev. D, 62, 103511

Meyer F., 2004, Prog. Theor. Phys. Suppl., 155, 45

Mii H., Totani T., 2005, ApJ, 628, 873

Miller M. C., Colbert E. J. M., 2004, Int.J.Mod.Phys., D13, 1

Niemeyer J. C., Jedamzik K., 1998, Phys. Rev. Lett., 80, 5481

Niemeyer J. C., Jedamzik K., 1999, Phys. Rev. D, 59, 124013

Okajima T., Ebisawa K., Kawaguchi T., 2006, ApJ, 652, L105

Omukai K., Tsuribe T., Schneider R., Ferrara A., 2005, ApJ, 626, 627

Ptak A., Griffiths R., 1999, ApJ, 517, L85

Ricotti M., Ostriker J. P., Mack K. J., 2008, ApJ, 680, 829

Schneider R., Ferrara A., Natarajan R., Omukai K., 2002, ApJ, 571, 30

Shtanov Y., Traschen J. H., Brandenberger R. H., 1995, Phys. Rev. D, 51, 5438

Spergel D. N. et al. [WMAP Collaboration], 2007, ApJS, 170, 377

Strohmayer T. E., Mushotzky R. F., 2003, ApJ, 586, L61

Strohmayer T. E., Mushotzky R. F., Winter L., Soria R., Uttley P., Cropper M., 2007, ApJ, 660, 580

Takeda M. et al., 2003, Astropart. Phys., 19, 447

Tetradis N., 1998, Phys. Rev. D, 57, 5997

Vierdayanti K., Mineshige S., Ebisawa K., Kawaguchi T., 2006, PASJ, 58, 915

Wright E. L., Reese E. D., 2000, ApJ, 545, 43

Yamaguchi M., 2001, Phys. Rev. D, 64, 063503

Yamaguchi M., Yokoyama J., 2003, Phys. Rev. D, 68, 123520

Yamaguchi M., Yokoyama J., 2004, Phys. Rev. D, 70, 023513

Yokoyama J., 1997, A&A, 318, 673

Yokoyama J., 1998a, Phys. Rev. D, 58, 083510

Yokoyama J., 1998b, Phys. Rep., 307, 133

Yokoyama J., 1998c, Phys. Rev. D, 58, 107502

Zezas A., Fabbiano G., Rots A. H., Murray S. S., 2002, ApJ, 577, 710